Materials Research. 2015; 18(4): 698-705
DOI: http://dx.doi.org/10.1590/1516-1439.342814
© 2015

Geopolymer/PEG Hybrid Materials Synthesis and Investigation of the Polymer Influence on Microstructure and Mechanical Behavior

Michelina Catauro[a]*, Ferdinando Papale[a], Giuseppe Lamanna[a], Flavia Bollino[a]

[a]Department of Industrial and Information Engineering, Second University of Naples, via Roma 29, Aversa (CE), Italy

Received: October 27, 2014; Revised: June 12, 2015

Geopolymers are aluminosilicate inorganic polymers, obtained from the alkali activation of powders containing SiO_2+Al_2O_3>80wt%, mainly proposed as environmentally friendly building materials. In this work, metakaolin-based geopolymers have been prepared and a water-soluble polymer, polyethylene glycol (PEG), has been added in different percentages to obtain organic-inorganic hybrid geopolymers. The influence of both the polymer amount and aging time on the structure and the mechanical behavior of the materials were investigated. FTIR spectroscopy allowed us to follow the evolution of the aluminosilicate framework during the geopolymerization process. This analysis revealed that PEG leads to a network which is rich in Al-O-Si bonds and forms H-bonds with the inorganic phase. SEM microscope showed that the two phases are interpenetrated on micrometric scales. Traction and bending tests have been carried out on appropriate samples to investigate the mechanical behavior of the obtained hybrids, showing that both PEG content and aging time affect the material behavior.

Keywords: *PEG/geopolymers hybrid, mechanical testing, chemical characterization*

1. Introduction

Geopolymers are amorphous, three-dimensional alkali aluminosilicate binder materials synthesized by means of the alkaline activation of clays, calcined clays, natural minerals, industrial waste, fly ash and other aluminosilicate sources[1,2]. A strong alkaline solution induces the dissolution of those solid raw materials producing aluminate and silicate species which link by means of a polycondensation reaction to form the 3D-cross-linked polysialate structure $([-(Si\text{-}O)_z\text{-}Al\text{-}O\text{-}]_n)$[3,2].

These materials were first introduced as calcium-free inorganic cements by Davidovits in 1978[4] and since then they have been attracting increasing attention due to their promising characteristics. They have been mainly proposed as more environmentally friendly substitutes of Portland cement[5,6] because of the greater energy efficiency of their manufacturing process and the substantial reduction in CO_2 emissions[7,8].

Following the particular aluminosilicate precursor[3], the stoichiometric ratio of Si/Al[1,9], alkali hydroxide and water content[10,11] as well as the reaction temperature, pressure[3], activation, setting and curing procedures[11,12], geopolymers can exhibit a wide variety of properties, such as high compressive strength, low shrinkage, fast or slow setting, acid and fire resistance, low thermal conductivity, long term durability and thermal stability. Thanks to these characteristics, geopolymers have a wide range of potential applications in construction building, in the biomedical field, in cultural heritage maintenance and renovation and immobilization of heavy metals and nuclear waste management.

*e-mail: michelina.catauro@unina2.it

Each of those applications require different mechanical properties, so the need to modulate them has induced many research groups to study how the variation of synthesis parameters influence the mechanical behavior of the geopolymer materials.

Duxson et al.[1] observed a microporous framework, with the pore size determined by the nature of lkali cations or mixture of cations used in activation; they worked studying the effects of the variation of Si/Al ratio and showed that for Si/Al $\leq$ 1.40 their specimens showed a microstructure comprising clustered dense particulates with large interconnected pores, while if Si/Al $\geq$ 1.65 the same microstructure appeared homogeneous with a porosity distributed in small pores, largely below the limits of observation in SEM micrographs, while Young's modulus showed a maximum value, denoting its dependence on homogeneity; the compressive strength increased in correspondence to larger Si/Al values, but then it would begin to decrease, and the authors pointed out that the observed effect was to be attributed to the presence of unreacted material, which played the role of a defect in the binder phase. Moreover, Burciaga-Diaz et al.[13] showed that an interesting increase in compression strength can be obtained by using geopolymers with a low content of metakaolinite, obtaining a product made of amorphous silicoaluminate intermixed with silica gel; they also defined some optimal ratios to increase strength in terms of SiO_2/Al_2O_3 and Na_2O/Al_2O_3 and determined the best curing conditions (24 h at 80 °C) to obtain a quick strength gain at an early maturation stage, even if for time-delayed uses the best curing conditions were found at 20 °C.

Geopolymers can also absorb different materials such as sand in their network, thus acquiring new behavioral advantages, or can be reinforced with carbon fibers or even with stainless steel meshes. Steinerova[14] tested geopolymer mortars with the addition of sand in the 0-93 wt% range; she found that at low contents of sand, the geopolymer's mechanical behavior worsened, because many cracks appeared in the matrix, starting from large pores of 1-8 μm; when the content of sand increased, the grains were able to block the cracks and higher mechanical properties were detected in those conditions; the best results were found for a sand content ranging 74-78 wt%, mainly because of the lack of large voids due to packing. In that range flexural strengths up to 4 MPa were measured, with a Young modulus of about 1.9 GPa.

A promising strategy to modify several properties of ceramic materials, including mechanical ones, applied even to geopolymers, is to add a polymeric phase to the inorganic matrix in order to develop an organic-inorganic hybrid nanocomposite[15-19]. This is a biphasic material where the components usually interpenetrate on scale of less than 1μm[20] and whose properties are not just the sum of the individual contributions of both phases, but derive from a great synergic effect between the single constituents. The nature of the bonds present between the phases has an impact on the properties of those materials. Therefore, Judeinstein & Sanchez[21] proposed a classification of the hybrids based on the interactions between the organic and the inorganic component. They defined those materials as first class hybrids, if they were characterized by weak bonds (hydrogen bond, Van der Waals forces, etc.) between the two phases, or second class hybrids, if strong bonds (covalent bond or ionic-covalent bond) occurred. In literature, numerous works describe the use of FT-IR spectroscopy and solid-state ^{13}C NMR techniques to study the interaction in biphasic systems. Wang et al.[22] demonstrated the formation of hydrogen bonds between the hydroxyl groups of poly(4-vinylphenol) and the poly(ε-caprolactone) (PCL) carbonyl using ^{13}C NMR[22]. Both static and CP-MAS ^{13}C NMR and FT-IR were used to investigate the interactions that occur in numerous hybrids nanocomposite materials between different polimers and several inorganic matrices (e.g. $CaCO_3$[23], CaO and/or SiO_2[24-29], TiO_2[30,31], ZrO_2[24,32-35]).

Zhang et al.[19] added to the uncalcined-kaolinite geopolymeric matrix some organic polymers (1 wt %) characterized by carboxyl or amino groups or even hydroxide radicals; in particular, they used polyacrylic acid, sodium polyacrylate, polyethylene glycol, polyvinyl alcohol and polyacrylamide, increasing the compressive strength of the mere inorganic polymer up to 29%; still larger increases were obtained for bending, up to about 65%, but in any case that resistance is characterized by very low values. In that way crack propagation resistance is increased by a bridging action which prevents the matrix from cracking. Ferone et al.[17] obtained significantly enhanced compressive strengths and toughness compared to the mere geopolymer by adding epoxy based organic resins to the geopolymeric matrix.

In the present work the authors have prepared novel organic-inorganic hybrid materials consisting of an inorganic matrix of a metakaolin-based geopolymer in which the polyethylene glycol (PEG), a water-soluble polymer commercially used as a plasticizer, were added in weight percentages of 3 and 6 wt%. The synthesized systems have been chemically characterized by FT-IR and SEM analyses and the influence of the aging time and of the polymer amount on the microstructure and the mechanical behavior have been investigated; thus all results have been reported as a function of those two parameters.

2. Material and Methods

2.1. Geopolymer preparation

The synthesized organic-inorganic hybrid materials consist of an inorganic metakaolin-based geopolymeric matrix in which different percentages of polyethylene glycol (PEG), were incorporated. Three different formulations of hybrids were prepared as shown in Table 1.

Metakaolin (MK) was used as the principal source of aluminosilicate, because it is the cheapest aluminosilicate with a good degree of purity. Moreover, this raw material improves the mechanical strength and reduces the transport of water and salts in the final product. The composition of the metakaolin used (Neuchem s.r.l) is reported in Table 2.

The metakaolin was sieved to obtain a fine powder with an average diameter of 80 μm. The powder was added gradually to an alkaline solution previously prepared by mixing of a sodium silicate solution, with ratio $SiO_2/Na_2O = 2.5$ (Sigma Aldrich, Milano, Italy), and sodium hydroxide pellets (Sigma Aldrich, Milan, Italy) with ratio $Na_2SiO_3/NaOH = 2.0$. The final composition of the geopolymer synthesized can be expressed as Al_2O_3 $3.4SiO_2$ $0.9Na_2O$ $11H_2O$.

To synthesize Geopolymer/PEG hybrid systems, PEG 400 (Sigma Aldrich, Milano, Italy) was also added in part to the alkaline solution and in part slowly together with metakaolin during the mixing phase. Resulting slurries were stirred mechanically for about 20 min at 750 rpm to reach good homogenization and then were poured in plexiglass clad moulds and sealed. The moulds were placed in an oven for 24 hrs at 45 °C (not greater as is usually done, as this temperature was sure to avoid any possible thermal degradation of the polymer) and successively stored for 28 days at room temperature.

2.2. Geopolymers characterization

The PEG presence in the samples and the kind of the bonds between organic and inorganic components in the hybrid materials were verified by Fourier transform infrared spectroscopy (FT-IR). FTIR transmittance spectra were recorded

Table 1. Formulation of the three geopolymers prepared for the study.

Samples Name	PEG Percentages (wt%)
GP0	0
GP3	3
GP6	6

Table 2. Metakaolin composition.

Al_2O_3	SiO_2	K_2O	Fe_2O_3	TiO_2	MgO	CaO
41.90%	52.90%	0.77%	1.60%	1.80%	0.19%	0.17%

in the 400-4000 cm^{-1} region using a Prestige 21 Shimatzu, Japan, system, equipped with a DTGS KBr -Deuterated Tryglycine Sulphate with potassium bromide windows detector, with resolution of 2 cm^{-1} (45 scans). The spectra of all prepared hybrid systems were registered at different aging times (7, 14 and 28 days) to follow the evolution of the aluminosilicate framework during the geopolymerization process and to assess the stability of the obtained matrices. KBr pelletised disks containing 2 mg of the sample and 198 mg KBr were prepared. FTIR spectra were elaborated by Prestige commercial software (IRsolution).

The morphological characterization, as a function of both aging time and polymer amount, was carried out using a scanning electron microscope (SEM, FEI Quanta 200) equipped with energy dispersive spectroscopy (EDS) after fixing the samples on stubs with colloidal graphite.

2.3. Mechanical tests

The produced paste was poured in a mold - coated with plexiglass to get an uniform surface - and two groups of samples were obtained to carry out the traction and bending tests; each group was composed of six specimens 36×40×160 mm size.

The tests were carried out by means of a Zwick-Roell® Z250 electromechanical testing machine, equipped with a data acquisition system mod. Spider-8 HBM®. The tests were performed in displacement control mode at a constant loading velocity and no preload, with environmental conditions T = 23 °C and 65% relative humidity; they were stopped after obtaining a minimum of 5 valid tests for each chemical concentration and aging time. Two different kinds of mechanical tests were conducted: the first one was a uniaxial compressive test and was performed at a 3 mm/min loading velocity, positioning the specimens between two compression plates. The plate surfaces were planar, parallel, smooth and extremely rigid and had a greater contact area than the specimen.

The second test was a three point bending flexural test. It can provide values for the modulus of elasticity, flexural stress, flexural strain and the flexural stress-strain response of the material. Great attention was paid to the loading velocity because the results of such kind of test are sensitive to this parameter. By means of dedicated preliminary tests the loading velocity was fixed to a value of 1 mm/min.

3. Results and Discussion

3.1. Geopolymer characterization

Figure 1 shows MK FTIR spectrum (curve a) compared with FTIR spectra of GP0 (i.e. geopolymer with 0% PEG) sample after 7, 14 and 28 days of aging (curves from b to d). All spectra contain broad absorption bands at about 3440 and 1650 cm^{-1} resulting from hydration water. Those peaks increase in the time because of the water formation as product of geoplymerization process. The MK spectrum shows sharp peaks at about 3695-3660 cm^{-1} and a weaker band at 912 cm^{-1}, ascribed to hydroxyl groups and Al(VI)-OH stretching vibrations in the kaolinite[36], indicating an incomplete conversion from kaolin to metakaolin ascribable to the calcination process. However, the presence of the band at about 798 cm^{-1}, due to Al(VI)-O stretching, which is absent in the kaolin spectrum, proves that the conversion occurred. Moreover, the strongest vibrations typical of all aluminosilicates (see Table 3), which are assigned to internal vibrations of Si-O-Si and Si-O-Al, are visible, such as the strong Si-O-Si asymmetrical stretching and bending vibrations, at about 1080 cm^{-1} and at about 430-460 cm^{-1}[37-39] respectively, and Al-O-Si bending vibrations at about 540 cm^{-1}.

In the spectra of the geopolymer recovered at different aging times the kaolinite bands disappear and a shift of the Si-O-Si band at lower wavenumber (after 28 days, it appears at about 1050 cm^{-1}) is observed, due to the increase of Si-O-Al bonds; an approximate relationship, indeed, between the frequency of the absorption bands and the ratio of Si:Al in the alluminosilicate framework was observed: the higher the Al inclusions, the lower the wave-length[40]. The increase of Si-O-Al bonds is also confirmed by the appearance in the GP0 spectrum of the peak at 1000 cm^{-1} after 7 days of aging, which shifts at 980 cm^{-1} after 28 days. The shift of that band is a consequence of the aluminosilicate framework reorganization which occurs due to the geopolymerization reactions and which is proved also by the appearance of some weak bands in the region of bending modes of the Si-O-Si and Si-O-Al bonds (800-430 cm^{-1})[37,38]. Moreover, in all GP0 spectra a weak band at 1454 cm^{-1},which increases with aging time (from curve b to c) is visible. That can be ascribed to Na_2CO_3 due to unreacted NaOH which was carbonated by atmospheric CO_2[41].

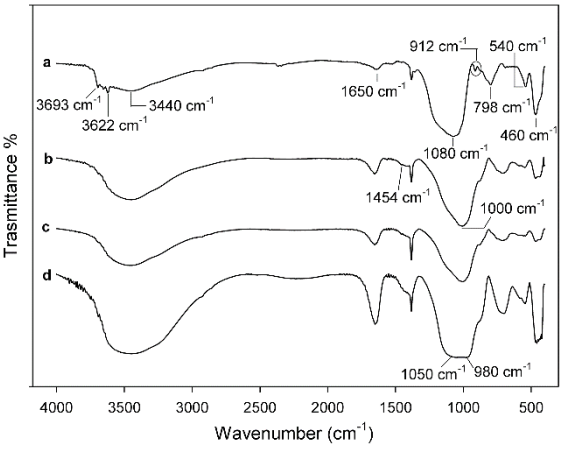

Figure 1. (a) MK FTIR spectrum compared with FTIR spectra of GP0 after (b) 7 days (c) 14 days and (d) 28 days.

Table 3. IR characteristic bands and their interpretation.

Absorption Bands	Interpretation
3695-3660 cm^{-1}	hydroxyl groups in the kaolinite
3450 and 1650 cm^{-1}	hydration water
1454 cm^{-1}	Na_2CO_3
1080-1050 cm^{-1}	Asymmetrical Si-O-Si stretching vibration
1010-980 cm^{-1}	Si-O-Al stretching vibration
912 cm^{-1}	Al(VI)-OH stretching
800-500 cm^{-1}	Al-O-Si bending vibrations
450-470 cm^{-1}	Si-O-Si bending vibrations

The same changes are observed comparing the spectra of GP3 or GP6 (geopolymers with PEG 3 and 6 wt% respectively) at different aging times. For those samples the band related to Si-O-Si stretching, visible at 1080 cm^{-1} in the MK spectrum and at 1050 cm^{-1} in the spectrum of GP0 recovered after 28 days, disappears and only the Al-O-Si band at 1000 cm^{-1} is visible, as shown in Figure 2, where FTIR spectra of MK (curve a) and GP3, 7, 14 and 28 days after the synthesis (curve from b to d) are reported as an example. Such result suggests that the polymer affects the geopolymerization reactions and induces a modification of the system evolution because it causes the formation of a greater number of Si-O-Al bonds in the aluminosilicates framework.

Figure 3 shows FTIR spectrum of PEG (curve d) compared with spectra of GP0, GP3 and GP6 (curve from a to c) samples. In the spectra of the hybrid systems (GP3 and GP6), the band at 2928 peculiar to symmetric stretching of -CH_2- of PEG, is visible and the peak's intensity increases with the amount of polymer. In the spectrum of GP6 a low intensity shoulder at about 1250 cm^{-1} also appears due to C-O ethereal

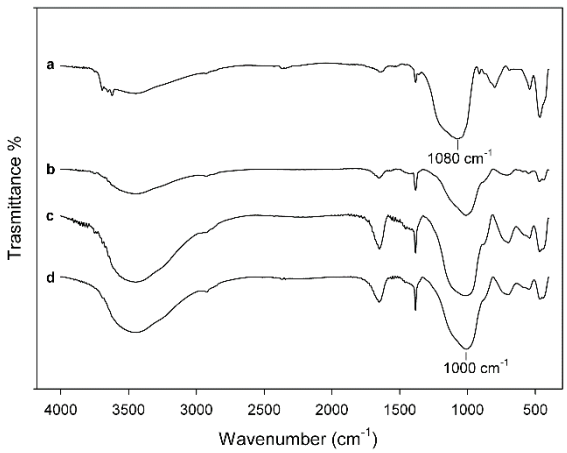

Figure 2. (a) MK FTIR spectrum compared with FTIR spectra of GP3 after (b) 7 days (c) 14 days and (d) 28 days.

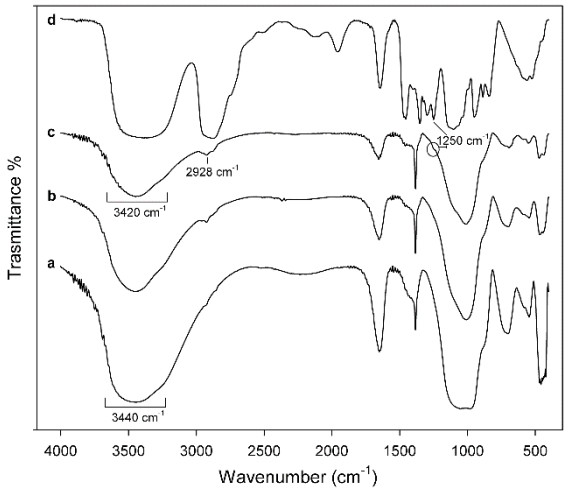

Figure 3. FTIR spectra of (a) GP0, (b) GP3, (c) GP6 after 28 days and (d) pure PEG.

groups in the polymer chains. Those observation confirms the presence of the organic phase in the geopolymeric matrix. Moreover, the change in the shape of the band at 3440 cm^{-1} (-OH stretching region) and its shift to low wavenumber (about 20 cm^{-1}) suggest the formation of new hydrogen bonds probably between the hydroxyl groups of the inorganic network and the oxygen ethereal or alcoholic groups of the PEG chains, which are able to give such interactions[24]. This is supported by the presence, in GP6 spectrum of a shoulder at 1250 cm^{-1} instead of a sharp peak, as it appears in pure PEG spectrum. Indeed, this means that the ethereal groups are involved in interactions and, thus, a peak broadening occurs. The obtained materials, thus are Class I hybrids in agreement with Judeinstein & Sanchez[21].

SEM analysis was performed on all hybrid formulations after 7, 14 and 28 days (Figure 4) and morphological differences depending on aging times only for GP0 were recorded. In particular, 7 days after the synthesis, GP0 appears compact and EDS analysis confirms that it has the calculated geopolymer composition, indicating that most of the metakaolin had already reacted (Figure 4a). However, at high magnifications some small areas (about 5 μm) can be observed, with the typical fibrous morphology of the unreacted MK, as confirmed by EDS (Figure 4b) where a lower Na content and Si/Al ratio is recorded compared to EDS in Figure 4a[42]. GP0 after 28 days (Figure 4c) appears more homogeneous and without unreacted metakaolin areas. EDS analysis was performed randomly on the sample confirming those conclusions.

After 28 days, the clarification of the air exposed surfaces of all samples is visible to the naked eye and SEM micrographs highlight the formation of needle-like crystals. The crystals' shape and their EDS spectra, where a high presence of O and Na was detected (Figure 4d), suggest that they are Na_2CO_3 crystals. That hypothesis is supported by the presence of the band at 1454 cm^{-1} in the IR spectra of all samples.

Figure 5 shows the geopolymer's morphology after 28 days as a function of the polymer amount. GP0 has a compact structure while GP3 and GP6 are porous and porosity increases as the percentage of PEG increases. The cavities are due to the removal of the polymer particles which occurred when the hybrid samples were subjected to SEM high vacuum. Their dimension (and thus PEG particles size) is in the range of 1-10 μm and no agglomeration phenomena were detected in the samples.

3.2. Mechanical testing

As reported, the compression and bending tests were performed on a Zwick-Roell® Z250 electromechanical testing machine in displacement control mode at a constant loading velocity and no preload on 36x40x160 mm specimens, with environmental conditions T = 23 °C and 65% relative humidity.

Four types of specimens were preliminarily tested, with different shape and size to verify the influence of a possible internal porosity. No significant differences were recorded, which allowed to assume a global equivalence with the adopted specimen dimensions.

As a representative sample of the obtained results, in Figure 6 a stress-strain plot is illustrated that shows the results obtained for 6% PEG from the uniaxial compression

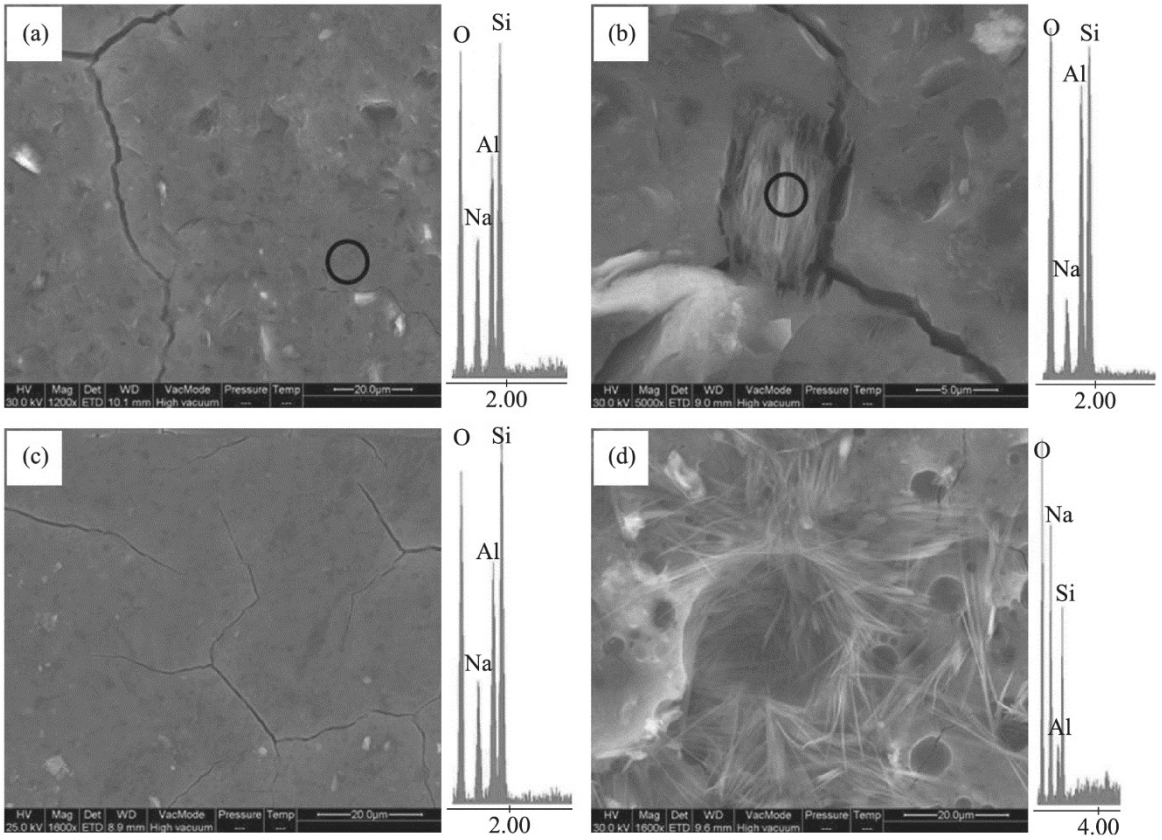

Figure 4. SEM micrograph and EDS analysis. (a) GP0 after 7 days and EDS performed on an reacted area (indicated in circle). (b) non-reacted metakaolin fibrous structure in GP0 after 7 days and EDS analysis. (c) GP0 after 21 days and EDS analysis performed randomly on surface. (d) SEM micrograph of crystals found on air exposed surface and their EDS spectra.

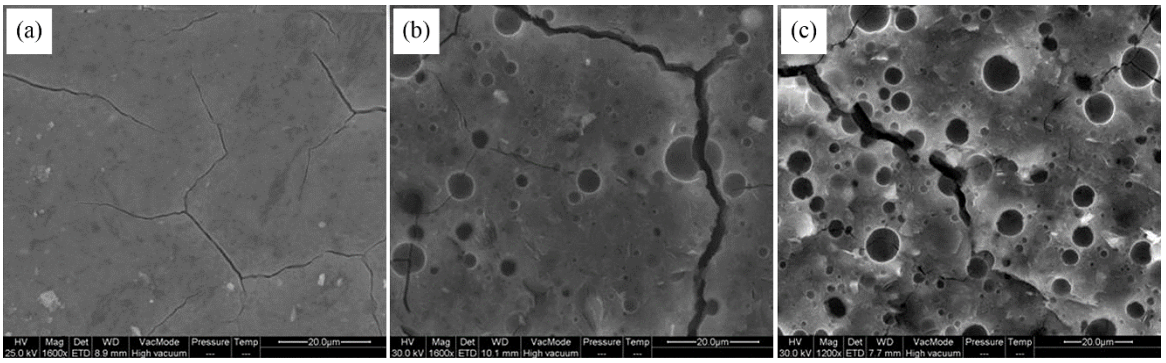

Figure 5. SEM micrographs of (a) GP0, (b) GP3 and (c) GP6 after 28 days.

test at different aging times. It can be observed an increase of Young modulus with aging time, less evident in the first two weeks and more evident during the subsequent aging period reaching up to 1.85 GPa after 14 days (+6.5% respect to 7 days aging) and 1.91 GPa after 28 days (+9.5% respect to 7 days aging). The same figure also shows an increase of the material's compressive strength with aging time up to 48.1 MPa after 14 days (+10% respect to 7 days aging) and 52.5 MPa after 28 days (+20% respect to 7 days aging). The combination of the latter effects with the flexural properties, described below, make the geopolymer very interesting for construction applications.

The results obtained for the three point bending flexural tests are shown in Figure 7; the three curves represent the experimental results for 6% PEG at different aging time. The aging globally issues greater strength and stiffness to the geopolymer: in fact, according to the results obtained for the compressive test, an increase of the ultimate bending stress can be observed up to 2.47 MPa (+7.6% respect to 7 days aging) and 2.87 MPa after 28 days (+25% respect to 7 days aging). As to the Young Modulus in bending, for a fixed quantity of polymer, it arises with aging up to 1.17 GPa (+14% respect to 7 days aging) and 1.70 GPa after 28 days (+65% respect to 7 days aging). Obviously we have to

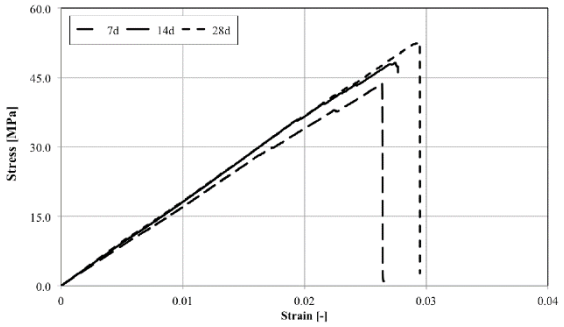

Figure 6. Compression stress vs. strain at different aging period (PEG 6 wt%).

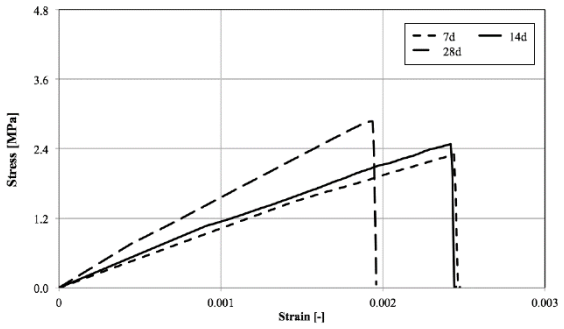

Figure 7. Bending stress vs. strain at different aging period (PEG 6 wt%).

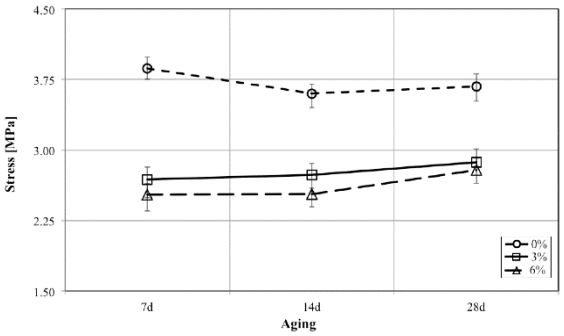

Figure 8. Bending strength vs. aging at different PEG percentages.

underline the remarkable difference between the compressive and the flexural strength. As reported in literature, bending behavior is driven by strains whose ultimate values are much lower, because of their variation in the section which classifies those materials as very brittle.

Among the obtained results the Authors have chosen to show those reported in the Figure 8 where the ultimate flexural stress is reported for all the tested configurations. In particular the plot reports the mean values of the five specimens for each of the nine combinations (aging time and percentage of PEG). For 3% and 6% PEG the ultimate flexural stresses increase with the aging time. Such an effect was reported in detail previously for 6% PEG but it appears evident also for 3% PEG. GP0 (i.e. geopolymer PEG-free) has a quite different behavior: it changes the trends compared to the others and it remains nearly constant as the aging time increases. That latter effect is probably due to a faster homogenization process of the material which occurs in PEG-free samples. On the contrary, when a percentage of PEG (3% and 6%) is added to the geopolymer, more time is required to reach the definite mechanical strength.

4. Conclusions

In this paper the synthesis of Class I hybrid geopolymers from metakaolin, obtained by adding different percentages of PEG, has been presented and the influence of both the aging time and the polymer amount on the microstructure and mechanical behavior of the obtained materials was assessed by means of FTIR, SEM analyses and mechanical tests, whose results were reported as function of those parameters.

The FTIR spectra have shown that the PEG is present in the hybrid formulations and suggest that the two hybrid components are bounded by means of H-bonds between -OH groups of the geopolymer inorganic matrix and the ethereal oxygen atoms and/or terminal alcoholic groups in the PEG chain. Moreover, they have shown that, in the time, the inorganic network is subjected to reorganization which causes an increase of Al-O-Si bonds because the geopolymerization reaction proceeds. The presence of PEG influences the reactions' evolution and causes the formation of an aluminosilicate framework which is reach in Si-O-Al bonds. However, the maturation of all samples occurs after 28 days.

The mechanical tests which have been carried out showed that by varying the formulation of hybrids corresponding different morphology and mechanical behavior are obtained.

SEM analysis proved that the PEG particles are dispersed in the inorganic matrix assuming a spherical shape with diameter in the range of 1-10 μm. the porosity is obviously more evident when 6% of PEG was added.

Also the mechanical behaviour of the materials is affected by the polymer. The evolution of the elastic modulus evaluated by a uniaxial compressive test and a three point bending flexural test is consistent with what was expected: the experimental results show a general increase of Young modulus with aging time, for a fixed percentage of PEG. On the other hand, the influence of PEG's percentage on the elastic properties could be better evaluated for an aging period of ninety days or longer. The results obtained in this work show a global increase of elastic strain for a fixed value of stress as the percentage of PEG increases but, in general, a decrease of flexural and compressive strengths.

It is also interesting to show how the polymer percentage influences the mechanical strength. In absence of PEG the experimental tests showed a global strength regularity with aging time due to the chemical composition of sample. PEG-free samples, indeed, can reach final mechanical resistance faster than hybrid systems. The stretching effect of PEG, that in general provides the characteristic of elasticity to the base material, together with the longer time required to reach the final structural strength justify the increase of flexural and compressive strengths with aging time.

Moreover, both the geopolymer formulations (3 and 6 wt% PEG) show the same slight slope of the curve strength vs aging time. Thus, it could be extremely interesting to study in a future work the minimum amount of PEG which causes that effect.

References

1. Duxson P, Provis JL, Lukey GC, Mallicoat SW, Kriven WM and van Deventer JSJ. Understanding the relationship between geopolymer composition, microstructure and mechanical properties. *Colloids and Surfaces. A, Physicochemical and Engineering Aspects*. 2005; 269(1-3):47-58. http://dx.doi.org/10.1016/j.colsurfa.2005.06.060.
2. Prud'homme E, Autef A, Essaidi N, Michaud P, Samet B, Joussein E, et al. Defining existence domains in geopolymers through their physicochemical properties. *Applied Clay Science*. 2013; 73:26-34. http://dx.doi.org/10.1016/j.clay.2012.10.013.
3. Duxson P, Fernández-Jiménez A, Provis JL, Lukey GC, Palomo A and van Deventer JSJ. Geopolymer technology: the current state of the art. *Journal of Materials Science*. 2007; 42(9):2917-2933. http://dx.doi.org/10.1007/s10853-006-0637-z.
4. Davidovits J. Geopolymers: inorganic polimeric new materials. *Journal of Thermal Analysis and Calorimetry*. 1991; 37(8):1633-1656. http://dx.doi.org/10.1007/BF01912193.
5. Duxson P, Provis JL, Lukey GC and van Deventer JSJ. The role of inorganic polymer technology in the development of 'green concrete'. *Cement and Concrete Research*. 2007; 37(12):1590-1597. http://dx.doi.org/10.1016/j.cemconres.2007.08.018.
6. Menna C, Asprone D, Ferone C, Colangelo F, Balsamo A, Prota A, et al. Use of geopolymers for composite external reinforcement of RC members. *Composites. Part B, Engineering*. 2013; 45(1):1667-1676. http://dx.doi.org/10.1016/j.compositesb.2012.09.019.
7. Ferone C, Colangelo F, Cioffi R, Montagnaro F and Santoro L. Use of reservoir clay sediments as raw materials for geopolymer binders. *Advances in Applied Ceramics*. 2013; 112(4):184-189. http://dx.doi.org/10.1179/1743676112Y.0000000064.
8. Habert G, d'Espinose de Lacaillerie JB and Roussel N. An environmental evaluation of geopolymer based concrete production: reviewing current research trends. *Journal of Cleaner Production*. 2011; 19(11):1229-1238. http://dx.doi.org/10.1016/j.jclepro.2011.03.012.
9. Ferone C, Colangelo F, Roviello G, Asprone D, Menna C, Balsamo A, et al. Application-oriented chemical optimization of a metakaolin based geopolymer. *Materials (Basel)*. 2013; 6(5):1920-1939. http://dx.doi.org/10.3390/ma6051920.
10. Jämstorp E, Strømme M and Frenning G. Modeling structure-function relationships for diffusive drug transport in inert porous geopolymer matrices. *Journal of Pharmaceutical Sciences*. 2011; 100(10):4338-4348. http://dx.doi.org/10.1002/jps.22636. PMid:21656516.
11. Catauro M, Bollino F, Papale F and Lamanna G. Investigation of the sample preparation and curing treatment effects on mechanical properties and bioactivity of silica rich metakaolin geopolymer. *Materials Science and Engineering C*. 2014; 36:20-24. http://dx.doi.org/10.1016/j.msec.2013.11.026. PMid:24433882.
12. Lancellotti I, Catauro M, Ponzoni C, Bollino F and Leonelli C. Inorganic polymers from alkali activation of metakaolin: effect of setting and curing on structure. *Journal of Solid State Chemistry*. 2013; 200(0):341-348. http://dx.doi.org/10.1016/j.jssc.2013.02.003.
13. Burciaga-Diaz O, Escalante-Garcia JI and Gorokhovsky A. Geopolymers based on a coarse low-purity kaolin mineral: Mechanical strength as a function of the chemical composition and temperature. *Cement and Concrete Composites*. 2012; 34(1):18-24. http://dx.doi.org/10.1016/j.cemconcomp.2011.08.001.
14. Steinerova M. Mechanical properties of geopolymer mortars in relation to their porous structure. *Ceramics-Silikáty*. 2011; 55(0):362-372.
15. Catauro M, Bollino F, Papale F, Giovanardi R and Veronesi P. Corrosion behavior and mechanical properties of bioactive sol-gel coatings on titanium implants. *Materials Science and Engineering C*. 2014; 43:375-382. http://dx.doi.org/10.1016/j.msec.2014.07.044. PMid:25175226.
16. Catauro M, Bollino F, Veronesi P and Lamanna G. Influence of PCL on mechanical properties and bioactivity of ZrO2-based hybrid coatings synthesized by sol-gel dip coating technique. *Materials Science and Engineering C*. 2014; 39:344-351. http://dx.doi.org/10.1016/j.msec.2014.03.025. PMid:24863235.
17. Ferone C, Roviello G, Colangelo F, Cioffi R and Tarallo O. Novel hybrid organic-geopolymer materials. *Applied Clay Science*. 2013; 73:42-50. http://dx.doi.org/10.1016/j.clay.2012.11.001.
18. Lamanna G, Soprano A, Bollino F and Catauro M. Mechanical characterization of hybrid (organic-inorganic) geopolymers. *Key Engeenering Materials*. 2013; 569-570:119-125. http://dx.doi.org/10.4028/www.scientific.net/KEM.569-570.119.
19. Zhang S, Gong K and Lu J. Novel modification method for inorganic geopolymer by using water soluble organic polymers. *Materials Letters*. 2004; 58(7-8):1292-1296. http://dx.doi.org/10.1016/j.matlet.2003.07.051.
20. McNaught AD and Wilkinson A. *Compendium of chemical terminology*. 2nd ed. Oxford: Blackwell; 1997.
21. Judeinstein P and Sanchez C. Hybrid organic-inorganic materials: a land of multidisciplinarity. *Journal of Materials Chemistry*. 1996; 6(4):511-525. http://dx.doi.org/10.1039/jm9960600511.
22. Wang J, Cheung MK and Mi Y. Miscibility and morphology in crystalline/amorphous blends of poly(caprolactone)/poly(4-vinylphenol) as studied by DSC, FTIR, and 13C solid state NMR. *Polymer*. 2002; 43(4):1357-1364. http://dx.doi.org/10.1016/S0032-3861(01)00673-5.
23. Ito T, Yamaguchi Y, Watanabe H and Asakura T. Structural analysis of oriented poly(ε-caprolactone) including CaCO3 particles with 13C solid-state NMR. *Journal of Applied Polymer Science*. 2001; 80(12):2376-2382. http://dx.doi.org/10.1002/app.1344.
24. Catauro M and Bollino F. Anti-inflammatory entrapment in polycaprolactone/silica hybrid material prepared by sol-gel route, characterization, bioactivity and in vitro release behavior. *Journal of Applied Biomaterials & Fundamental Materials*. 2013; 11(3):e172-e179. http://dx.doi.org/10.5301/JABFM.2012.9256. PMid:22798238.
25. Catauro M and Bollino F. Release kinetics of anti-inflammatory drug, and characterization and bioactivity of SiO2+PCL hybrid material synthesized by sol-gel processing. *Journal of Applied Biomaterials & Functional Materials*. 2014; 12(3):218-227. PMid:24425379.
26. Catauro M, Bollino F, Cristina Mozzati M, Ferrara C and Mustarelli P. Structure and magnetic properties of SiO2/PCL novel sol–gel organic–inorganic hybrid materials. *Journal of Solid State Chemistry*. 2013; 203:92-99. http://dx.doi.org/10.1016/j.jssc.2013.04.014.
27. Catauro M, Bollino F and Papale F. Synthesis of SiO2 system via sol-gel process: biocompatibility tests with a fibroblast strain and release kinetics. *Journal of Biomedical Materials Research. Part A*. 2014; 102(6):1677-1680. http://dx.doi.org/10.1002/jbm.a.34836. PMid:23776153.
28. Catauro M, Papale F, Roviello G, Ferone C, Bollino F, Trifuoggi M, et al. Synthesis of SiO2 and CaO rich calcium silicate systems via sol-gel process: bioactivity, biocompatibility, and drug delivery tests. *Journal of Biomedical Materials Research. Part A*. 2014; 102(9):3087-3092. http://dx.doi.org/10.1002/jbm.a.34978. PMid:24123774.
29. Catauro M, Bollino F, Papale F, Gallicchio M and Pacifico S. Synthesis and chemical characterization of new silica

polyethylene glycol hybrid nanocomposite materials for controlled drug delivery. *Journal of Drug Delivery Science and Technology*. 2014; 24(4):320-325. http://dx.doi.org/10.1016/S1773-2247(14)50069-X.

30. Catauro M, Bollino F, Papale F, Marciano S and Pacifico S. TiO2/PCL hybrid materials synthesized via sol-gel technique for biomedical applications. *Materials Science and Engineering C*. 2015; 47:135-141. http://dx.doi.org/10.1016/j.msec.2014.11.040. PMid:25492181.
31. Piccirillo AM, Borysenko SS and Borysenko SD. Qualitative analysis behaviour of the solutions of impulsive differential systems. *AAPP Atti della Accademia Peloritana dei Pericolanti: Classe di Scienze Fisiche, Matematiche e Naturali*. 2011; 89(2):C1A8902002-C1A8902002-12. http://dx.doi.org/10.1478/C1A8902002.
32. Catauro M, Bollino F, Papale F, Mozetic P, Rainer A and Trombetta M. Biological response of human mesenchymal stromal cells to titanium grade 4 implants coated with PCL/ZrO2 hybrid materials synthesized by sol-gel route: in vitro evaluation. *Materials Science and Engineering C*. 2014; 45:395-401. http://dx.doi.org/10.1016/j.msec.2014.09.007. PMid:25491844.
33. Catauro M, Bollino F, Papale F, Mozzati MC, Ferrara C and Mustarelli P. ZrO2/PEG hybrid nanocomposites synthesized via sol-gel: characterization and evaluation of the magnetic properties. *Journal of Non-Crystalline Solids*. 2015; 413:1-7. http://dx.doi.org/10.1016/j.jnoncrysol.2015.01.014.
34. Catauro M, Papale F, Bollino F, Gallicchio M and Pacifico S. Biological evaluation of zirconia/PEG hybrid materials synthesized via sol-gel technique. *Materials Science and Engineering C*. 2014; 40:253-259. http://dx.doi.org/10.1016/j.msec.2014.04.001. PMid:24857491.
35. Catauro M, Bollino F and Papale F. Biocompatibility improvement of titanium implants by coating with hybrid materials synthesized by sol-gel technique. *Journal of Biomedical Materials Research. Part A*. 2014; 102(12):4473-4479. PMid:24677575.
36. Tsai Y-L, Hanna JV, Lee Y-L, Smith ME and Chan JCC. Solid-state NMR study of geopolymer prepared by sol–gel chemistry. *Journal of Solid State Chemistry*. 2010; 183(12):3017-3022. http://dx.doi.org/10.1016/j.jssc.2010.10.008.
37. Frost RL, Fredericks PM and Shurvell HF. Raman microscopy of some kaolinite clay minerals. *Canadian Journal of Applied Spectroscopy*. 1996; 41(1):10-14.
38. Parker RW and Frost RL. The application of drift spectroscopy to the multicomponent analysis of organic chemicals adsorbed on montmorillonite. *Clays and Clay Minerals*. 1996; 44(1):32-40. http://dx.doi.org/10.1346/CCMN.1996.0440103.
39. Piccirillo AM, Ciarletta M and Borysenko SD. Impulsive wendroff's type inequalities and their applications. *AAPP Atti della Accademia Peloritana dei Pericolanti: Classe di Scienze Fisiche, Matematiche e Naturali*. 2012; 90(2):A2-1-A2-16. http://dx.doi.org/10.1478/AAPP.902A2.
40. Milkey RG. Infrared spectra of some tectosilicates. *The American Mineralogist*. 1960; 45:990-1007.
41. Gadsden JA. *Infrared spectra of minerals and related inorganic compounds*. London: Butterworths; 1975.
42. Williams RP, Hart RD and van Riessen A. Quantification of the extent of reaction of metakaolin-based geopolymers using X-ray diffraction, scanning electron microscopy, and energy-dispersive spectroscopy. *Journal of the American Ceramic Society*. 2011; 94(8):2663-2670. http://dx.doi.org/10.1111/j.1551-2916.2011.04410.x.